JP4.11 ALLOWING FOR INHOMOGENEOUS CLOUDS IN THE GODDARD EARTH OBSERVING SYSTEM GCM COLUMN RADIATION MODEL

L. Oreopoulos*[1,2], H. W. Barker[3], M.-D. Chou[2], R. F. Cahalan[2,1], and M. Khairoutdinov[4]

1. JCET– University of Maryland Baltimore County, Baltimore, MD
2. Laboratory for Atmospheres, NASA Goddard Space Flight Center, Greenbelt, MD
3. Meteorological Service of Canada, Downsview, ON
4. Dept. of Atmospheric Sciences, Colorado State University, Fort Collins, CO

1. INTRODUCTION

Our efforts focus on improving the solar radiative transfer calculations under cloudy conditions in NASA Goddard GCMs. Specifically, our goal is to apply a solar radiative transfer scheme which could potentially handle both subgrid horizontal and vertical cloud variability. This abstract describes recent progress in the implementation of an algorithm that accounts for horizontal cloud water variability in the solar code described by Chou et al. (1998). The modifications introduced are based on the ideas developed by Oreopoulos and Barker (1999).

2. CASCADE CLOUDS

It was rather straightforward to replace the standard delta-Eddington two-stream solutions for homogeneous clouds in the Chou et al. (1998) scheme with similar solutions integrated over a gamma distribution of optical depths (Oreopoulos and Barker 1999) under overcast conditions. An additional modification was the downward adjustment of optical depth for all but the first layer of contiguous vertically correlated (with respect to optical properties) clouds in order to implicitly account for the horizontal variability of radiation transmitted to layers below the topmost cloud layer (details are given in Oreopoulos and Barker 1999).

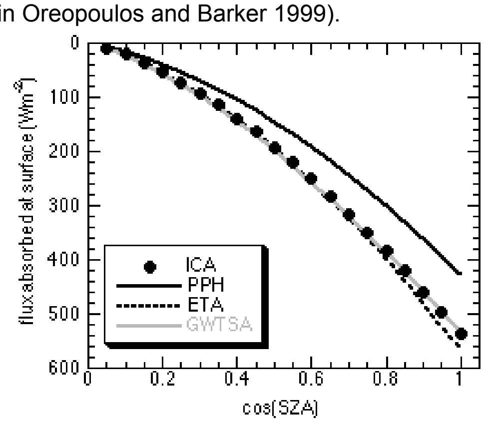

Figure 1 Broadband flux absorbed at surface as a function of solar zenith angle (SZA) for three different methods and the ICA benchmark. Surface albedo is 0.2 across the solar spectrum and the cloud embedded in the midlatitude summer (MLS) 75-layer atmosphere is described in the adjacent text.

* *Corresponding author address:* Lazaros Oreopoulos, NASA GSFC, Code 913, Greenbelt. MD, 20771; e-mail: lazaros@climate.gsfc.nasa.gov

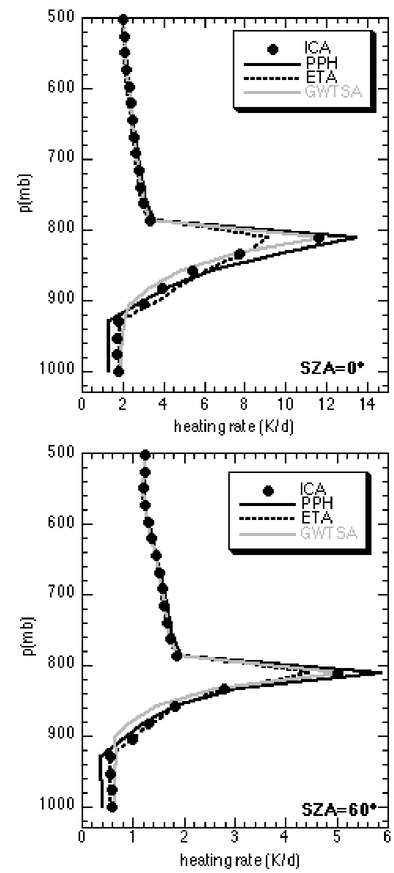

Figure 2 Broadband heating rates of the lower troposphere for SZA=0° (top) and SZA=60° (bottom). Same cloud as in Fig. 1. GWTSA performs better than ETA at the layer of maximum heating.

The easiest and quickest way to test the performance of the modified code (GWTSA) is to perform RT calculation on overcast cascade clouds generated as in Cahalan et al. (1994). Figure 1 shows the flux absorbed at the surface when five layers of contiguous cascade clouds with perfect vertical correlation of optical properties and a total visible optical thickness of ~15 and $\nu \equiv (\langle\tau\rangle/\sigma_\tau)^2 \approx 1$ are inserted between ~800 and ~917 mb in a MLS atmosphere. GWTSA is compared with homogeneous (PPH) and Effective Thickness Approximation (ETA) [Cahalan et al. 1994] and against the benchmark, the Independent Column Approximation (ICA). Figure 2 shows heating rate comparisons for SZA=0° and 60°.

GWTSA performs remarkably well, and while the improvement over ETA is small for fluxes, GWTSA has an edge in the heating rate comparisons. These results are consistent with previously published results in Oreopoulos and Barker (1999).

3. CRM RADIATION EXPERIMENTS

Experiments with overcast cascade clouds are not the most rigorous for assessing the quality of GWTSA: the optical depth distributions are well-described by gamma distributions, there are no cloud fraction overlap concerns, and the semi-empirical downward adjustment of optical depth takes advantage of the perfect vertical correlation. Much more can be learned, however, from applying the new scheme on complex convective cloud fields generated by a Cloud Resolving Model (CRM). Such a dataset simulating clouds for a week-long GATE period has been produced by M. Khairoutdinov. Water condensate fields are saved for every hour of simulation for a total of 164 cloudy snapshots.

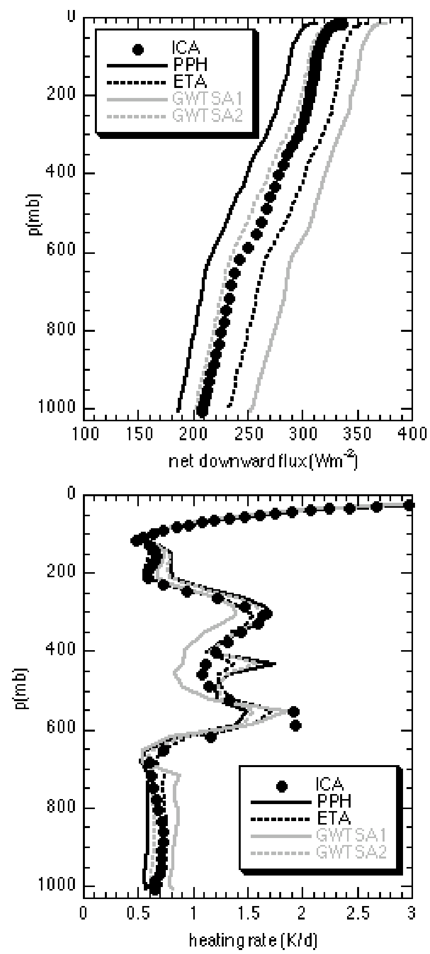

Figure 3 Broadband net downward flux (top) and heating rate (bottom) profiles for the benchmark (ICA) and several approximations as in Fig. 1 and 2. GWTSA1 is the standard GWTSA as in Oreopoulos and Barker (1999). For GWTSA2 the downward adjustment of optical depth has been removed.

Due to the significant computational time required to perform the ICA calculations and the desire to initially examine sensitivity to various minor algorithm modifications, we restricted the RT experiments to 20 fields and a single SZA (60°) only, at this time. These are the fields with index 51 to 70. Ensemble results for net downward flux and heating rate profiles are shown in Fig. 3, while Fig. 4 shows rms and mean errors relative to ICA. The line in Fig. 4 delineates calculations with and without the scaling of optical depth described by Chou et al. (1998). In the latter case the reflectance and transmittance of each layer was calculated as the weighted average of the clear and cloudy parts before being used in the radiative linking between layers, thus mimicking conditions of random overlap.

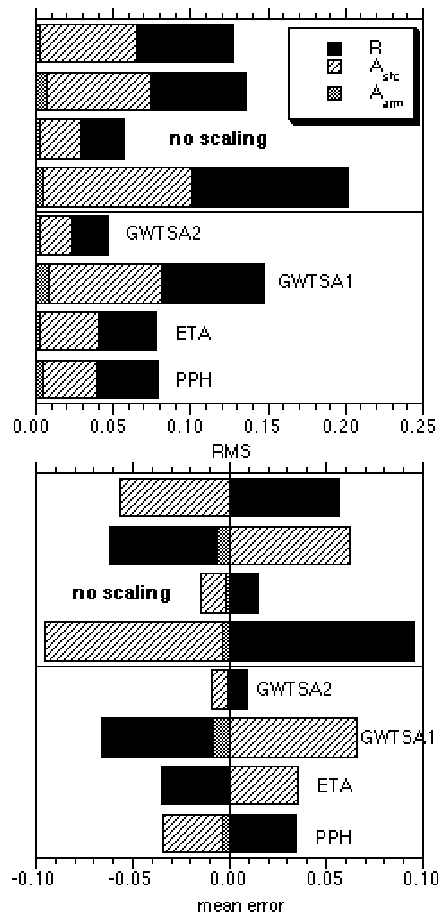

Figure 4 rms (top) and mean (bottom) error of various approximations with respect to ICA for albedo (R), surface absorptance (A_{sfc}), and atmospheric absorptance (A_{atm}). GWTSA1 and GWTSA2 are defined in Fig. 3. The meaning of “no-scaling” is described in the text. The order of bars above the separator line is the same as below the line.

4. DISCUSSION AND FUTURE WORK

Figures 3 and 4 show that removing the optical depth adjustment of Oreopoulos and Barker (1999) actually improves the overall performance of GWTSA. This suggests that vertical correlation of cloud water amounts is not as strong as implied by the scheme. Fig. 5 seems to support this. Hence, the empirical treatment of correlation may need to be modified. We plan to examine this issue more closely in the future. ETA does not perform significantly better than PPH whose smaller than expected errors should probably be attributed to the scaling of optical depth that is introduced to treat overlap, as described in Chou et al. (1998).

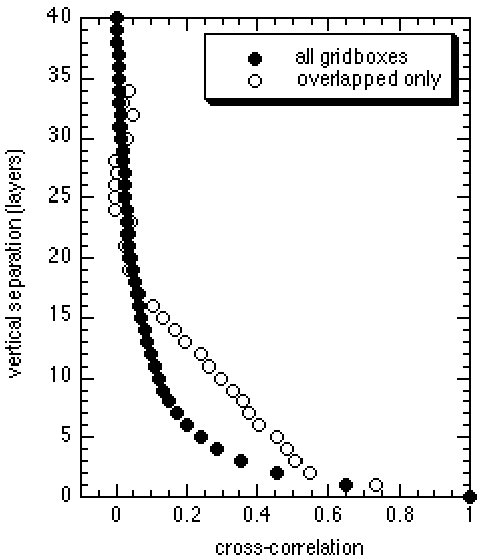

Figure 5 Ensemble average cross-correlation of layer total water fields as a function of their vertical separation.

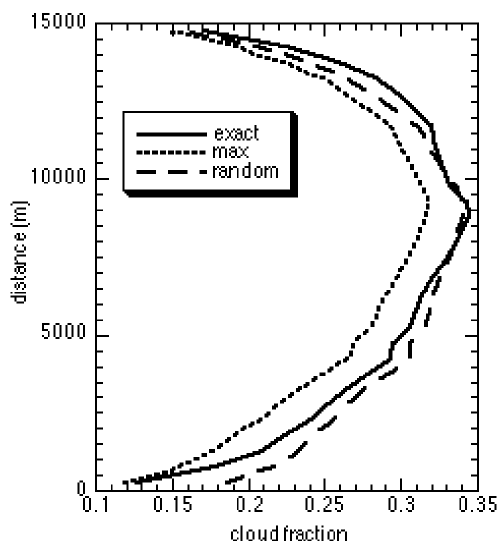

Figure 6 Ensemble average of combined cloud fraction of layer pairs as provided by the CRM fields (exact) and as calculated from the maximum and random overlap assumptions.

The experiments where the scaling was removed and the cloud overlap was modified to be essentially random, resulted in the deterioration of the overall performance, except for ETA (Fig. 4). This seems to suggest that the scaling à la Chou et al. (1998) takes care of some of the inhomogeneity and that further scaling according to ETA rules thins the clouds too much (note the negative mean error for R in Fig. 4b when the scaling is maintained).

We should also note that although we show results only for liquid droplet of r_{eff} =12 μm, we also performed experiments with mixed phase clouds and obtained qualitatively almost identical results.

Our future plan is to improve the performance of the algorithm by combining horizontal variability and vertical cloud overlap, in particular to incorporate into the scheme overlap functions such as those shown in Fig. 6. We also plan to evaluate our performance for the ICRCCM-III input dataset.

REFERENCES

Cahalan, R. F., W. Ridgway, W. J. Wiscombe, T. L. Bell and J. B. Snider, 1994: The albedo of fractal stratocumulus clouds, *J. Atmos. Sci.* **51**, 2434 - 2455.

Chou, M.-D., M. J. Suarez, C.-H. Ho. M. M.-H. Yan, and K.-T. Lee, 1998: Parameterizations for cloud overlapping and shortwave single-scattering properties for use in general circulation and cloud ensemble models, *J. Climate,* **11,** 202-214.

Oreopoulos, L., and H. W. Barker, 1999: Accounting for subgrid-scale cloud variability in a multi-layer 1D solar radiative transfer algorithm. *Q. J. Roy. Meteor. Soc.*, **126**, 301-330.